ELSEVIER

Journal of Alloys and Compounds 408–412 (2006) 496–502

Journal of ALLOYS AND COMPOUNDS

www.elsevier.com/locate/jallcom

Some major aspects of the chemical behavior of rare earth oxides: An overview

S. Bernal *, G. Blanco, J.J. Calvino, J.A. Pérez Omil, J.M. Pintado

Departamento de Ciencia de los Materiales, Ingeniería Metalúrgica y Química Inorgánica, Facultad de Ciencias, Universidad de Cádiz, Apartado 40, E-11510 Puerto Real, Cádiz, Spain

Received 30 July 2004; received in revised form 9 December 2004; accepted 15 December 2004
Available online 27 June 2005

Abstract

The chemical behavior of sesquioxides and higher rare earth oxides is briefly reviewed. In the first case processes implying no change in the lanthanoid oxidation state are considered, whereas in the second one the analysis is focused on their redox behavior.

Keywords: Rare earths oxides; Sesquioxides; Higher oxides; Acid–base behavior; Redox properties; Metal–rare earth oxide interaction phenomena

1. Introduction

As deduced from some recent review works [1] and specialized books [2,3] for the last 25 years, the research activity on different aspects of the structural, physical and chemical properties of the rare earth oxides has grown in a very impressive way. Formerly considered as a group of oxides with an interest largely localized in academic environments; these materials are presently finding very relevant technological applications. In some cases, these industrial uses imply large scale consumptions of them [2].

In recent years, an alternative procedure very much enhancing the classic wet technology for the separation of lanthanoid elements has been reported [4]. This finding may significantly lower the production costs of high purity rare earth oxides, thus favoring a rapid increase of both fundamental and applied research on these materials, and presumably, of their industrial uses [5].

In accordance with their relatively low atomization enthalpies and ionization potentials, the lanthanoid elements are acknowledged to be highly reducing elements, with electronegativities close to that of calcium [6]. In agreement with their successive ionization potentials [6], the (3+) oxidation state is a very characteristic chemical feature of these elements, the corresponding sesquioxides, Ln_2O_3, being known for all of them. In the case of Ce, Pr and Tb, three elements exhibiting a relatively low fourth ionization potential, the (4+) oxidation state is very relevant as well. Higher oxides, i.e. dioxides and mixed-valent (3+/4+) oxide phases, are therefore well known [1,7]. Thermochemical data corresponding to both rare earth sesquioxides and dioxides are reported in refs. [8,9].

Lower rare earth oxides, in which the lanthanoid elements show the (2+) oxidation state, are also known [1], those of Eu and Yb being the best characterized examples [1,10,11]. Their instability with respect of the sesquioxides makes their manipulation difficult, thus explaining the scarce chemical information existing about them.

This brief overview will be focused on the chemical behavior of the sesquioxides, Ln_2O_3, and the higher, fluorite-related, oxides, Ln_nO_{2n-2m}. Following the Johnson's proposal [12], two major categories of processes involving the rare earth oxides will be considered here, the reactions occurring with no change in the lanthanoid oxidation state, and those implying modifications of it.

Because of the high stability of the 3+ oxidation state in most of the lanthanoid elements, the typical reactions

* Corresponding author. Tel.: +34 956 016338; fax: +34 956 016288.
E-mail address: serafin.bernal@uca.es (S. Bernal).

0925-8388/$ – see front matter © 2005 Elsevier B.V. All rights reserved.
doi:10.1016/j.jallcom.2004.12.090

Table 1
Crystalline phases belonging to the Ln_2O_3–H_2O–CO_2 system

System	Phase	Remarks	Reference
Ln_2O_3–H_2O	$Ln(OH)_3$	Hexagonal except $Lu(OH)_3$	[15–17]
	LnO(OH)	Monoclinic	[15,18,19]
Ln_2O_3–CO_2	$Ln_2O_2CO_3$-I	Tetragonal	[15,20]
	$Ln_2O_2CO_3$-IA	Monoclinic	[15,20]
	$Ln_2O_2CO_3$-II	Hexagonal	[15,20]
Ln_2O_3–H_2O–CO_2[a]	$Ln_2(CO_3)_2{\cdot}3H_2O$	Orthorhombic	[21,22]
	$Ln_2(CO_3)_2{\cdot}3H_2O$	Orthorhombic	[21,22]
	$Ln(OH)(CO_3)$-A	Ancylite-like	[23,24]
	$Ln(OH)(CO_3)$-B	Bastnaesite-like	[25,26]
	$Ho_2(OH)_4(CO_3)$	Monoclinic	[27]

[a] X-ray diffraction data for several other phases belonging to this ternary system has been reported in [28].

involving the rare earth sesquioxides would belong to the first category above, i.e. acid–base processes. By contrast, the chemical behavior of the higher oxides would be characterized by processes included in the second category; i.e. redox reactions. Accordingly, this work has been organized in two major sections, the first one aimed at briefly reviewing some representative processes illustrating the acid–base properties of the rare earth sesquioxides; the second one being devoted to overview the redox behavior of the higher oxides.

2. Acid–base behavior of the sesquioxide phases (Ln_2O_3)

Before analyzing their chemistry, it is worth recalling a number of features characterizing the series of rare earth sesquioxides. They are made up by rather large cations, whose ionic radii smoothly decrease throughout the series [6]. Likewise, the difference in the electron configuration of the Ln(III) ions are associated with changes occurred in the inner relatively well screened from the chemical surroundings ($n-2$) 4f levels. Consistently, the bonding in this group of oxides is dominated by the ionic model [7], with rather minor contributions of the crystal field [13] and covalent effects. All these characteristics allow us to rationalize the acknowledged basic properties of the rare earth sesquioxides [14], and suggest a smooth and progressive decrease of this character throughout the series. Also related to these chemical characteristics, the lanthanoide sesquioxides exhibit a remarkable polymorphism. Five different structural varieties have been reported, three of them, those referred to as A (hexagonal), B (monoclinic) and C (cubic), being known to exist at ambient temperature and pressure [1].

In accordance with their basic character [7], the rare earth sesquioxides are active against H_2O and CO_2. Because of their special relevance, in this work, the attention will be focused on the processes occurring upon exposure to atmospheric CO_2 and H_2O, i.e. when aged in air, under the usual

Table 2
Water and carbon dioxide contents of aged-in-air rare earth sesquioxides

Oxide sample	S_{BET} ($m^2\ g^{-1}$)	Weight loss (%)		Molecules (nm^{-2})		Molar ratio	
		H_2O	CO_2	H_2O	CO_2	H_2O/Ln_2O_3	CO_2/Ln_2O_3
A-La_2O_3[a]	3.4	16.4	1.1	1372	38	3.00	0.07
A-La_2O_3[a]	5.2	15.7	1.5	859	34	2.77	0.11
A-La_2O_3[a]	16.3	14.2	2.8	250	20	2.57	0.21
A-Nd_2O_3[a]	5.9	13.3	2.3	717	51	2.49	0.18
A-Nd_2O_3[b]	6.4	15.0	2.5	289	20	2.86	0.17
A-Nd_2O_3[b]	2.2	15.3	2.2	389	23	2.86	0.17
C-Nd_2O_3[b]	5.0	12.4	2.2	696	50	2.32	0.17
C-Nd_2O_3[b]	17.4	12.3	2.8	226	21	2.30	0.21
B-Sm_2O_3[a]	6.4	15.6	1.6	696	29	3.00	0.12
C-Sm_2O_3[a]	8.2	4.9	1.7	187	28	0.93	0.14
C-Sm_2O_3[a]	14.9	6.3	3.2	130	27	1.23	0.25
C-Eu_2O_3[a]	25.6	10.6	2.0	111	9	2.08	0.16
C-Dy_2O_3[a]	22.3	5.4	2.5	74	14	1.12	0.21
C-Ho_2O_3[a]	32.5	3.2	2.6	30	10	0.67	0.22
C-Yb_2O_3[a]	40.0	6.4	4.6	48	14	1.40	0.40

Data as determined from thermogravimetric analysis (TG) or temperature programmed decomposition (TPD).
A, B, and C account, respectively, for the hexagonal, monoclinic or cubic structure of the starting sesquioxide sample [1].
[a]Data taken from [29].
[b]Data taken from [30].

storage and handling conditions. This information, in addition to be of interest for characterizing their chemical behavior, is critically important to properly use them as pure oxides, as components of multi-phase systems, or as starting reactant in the preparation of a variety of materials.

2.1. Aging-in air of rare earth sesquioxides: hydration and carbonation phenomena

As discussed in a recent review work [15], a wide variety of both amorphous and crystalline phases belonging to the Ln_2O_3–H_2O–CO_2 system have been reported in the literature. Table 1, summarizes the crystalline phases that are presently well-known for this system. Some of them have been observed to occur in the aged-in-air rare earth sesquioxides or, as intermediate phases, in their thermal decomposition.

Under the experimental conditions occurring in the air ($T = 298$ K, $P(CO_2) \approx 0.25$ Torr, and $P(H_2O) \approx 20$ Torr), all the rare earth sesquioxides are thermodynamically unstable against atmospheric H_2O and CO_2 [15]. The thermodynamic analysis suggests that the aged phases most likely would consist of hydroxycarbonates [15]. However, the experimental studies carried out on a wide series of rare earth oxides, Table 2, show a far more complex behavior.

As expected from thermodynamic considerations [15], data in Table 2 indicate that aging phenomena are much less strong on the heavier oxides. The hydration intensity varies in a much wider range than that of the carbonation process. The difference is particularly obvious if CO_2 and H_2O uptakes are referred to the surface area of the starting oxides. Carbonation is always a surface related phenomenon, whereas the hydration of the lighter members of the series, seems to be independent on their surface area.

In addition to the quantitative differences noted above, the analysis of the corresponding TG and TPD traces, and of X-ray diffraction (XRD) and infrared spectroscopy data recorded for the aged phases has allowed to distinguish three groups of sesquioxides (I–III) [29]. This proposal was later on confirmed by additional studies performed on some samaria [31] and neodymia [30,32] samples.

Group I would include hexagonal (A) samples and monoclinic samaria [15]. Though the aging rate decreases from lanthana through samaria, the intensity of aging is always high, implying the disappearance of the starting oxide. As revealed by the XRD and IR characterization studies, the hexagonal hydroxide, $Ln(OH)_3$, is the major component of the aged samples. No crystalline carbonates could be detected by XRD. This contrasts with the observations reported in [36], where a crystalline ancylite-like hydroxycarbonate phase is formed upon soaking lanthana in liquid water, at room temperature. The carbonation process occurring in Group I oxides exposed to the air is therefore different from that taking place when dispersed in water.

The carbonate phase resulting from the aging-in-air of Group I oxides consists of a few surface layers of a heavily disordered hydroxycarbonate-like phase surrounding a nucleus of crystalline hydroxide. This proposal is consistent with the results reported in Table 2, and the high resolution electron microscopy (HREM) images shown in Fig. 1.

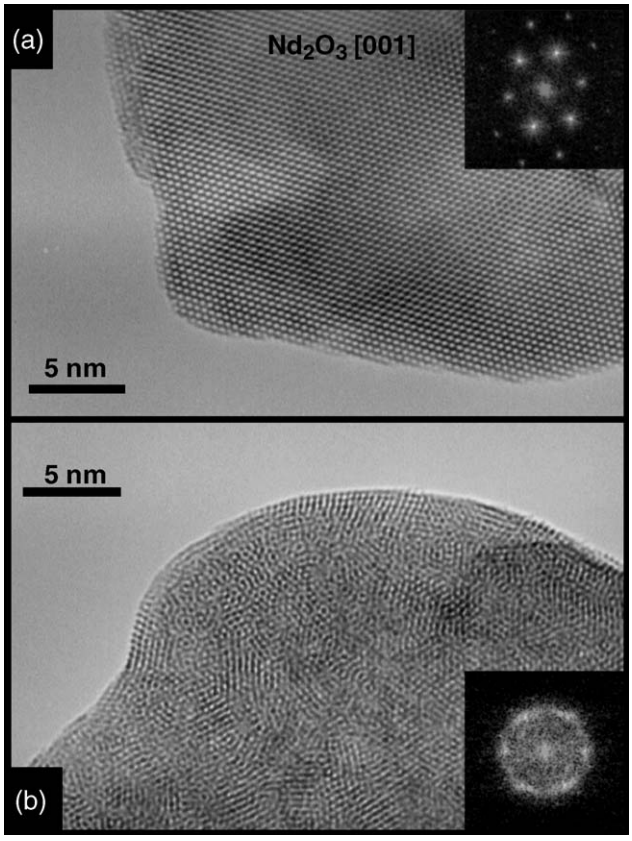

Fig. 1. HREM study of aging-in-air effects on Group I rare earth sesquioxides. Images corresponding to an hexagonal neodymia sample, fresh (a), and aged-in-air for 55 days (b).

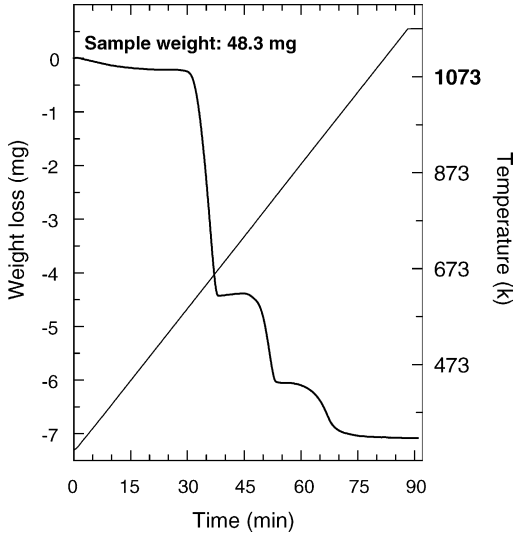

Fig. 2. Typical TGA diagram for an aged-in-air Group I oxide. Sample: lanthana.

In accordance with the thermogravimetric analysis (TG) diagrams recorded for Group I aged-in-air oxides, their thermal decomposition takes place through three well defined steps, Fig. 2. As revealed by parallel temperature programmed decomposition with analysis of the evolved gases by mass spectrometry (TPD-MS) studies [33], the first two steps mainly consist of dehydration processes, whereas CO_2 is the only gaseous product observed in the third one. For aged A-Nd_2O_3 and B-Sm_2O_3 these three steps are progressively and slightly shifted towards lower temperatures [15].

With the help of XRD and IR spectroscopy characterization studies performed on both the aged oxides and the intermediate phases resulting from their thermal decomposition, TG diagrams like that reported in Fig. 2 have been interpreted as follows [34]:

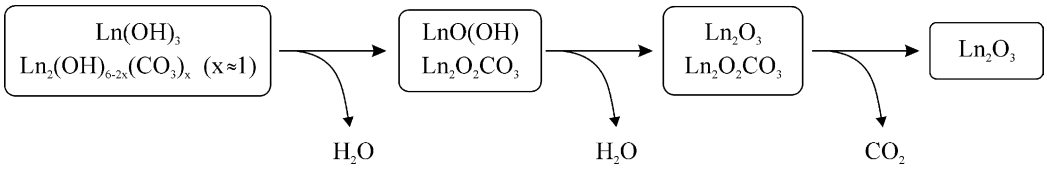

Group II would include the lighter cubic, C-type, oxides: neodymia, samaria and europia [15]. Typical TG and TPD diagrams for the aged oxides of this group are reported in [29]. As deduced from the IR spectroscopy [29,30] and XRD [30] data, the main structural feature characterizing these aged-in-air oxides is the presence of a crystalline hydroxycarbonate, which has been described as $Ln_2(OH)_4CO_3 \cdot nH_2O$. This hydroxycarbonate phase seems to be different from those reported in Table 1.

Group III would include the heaviest sesquioxides: Dy_2O_3, Ho_2O_3 and Yb_2O_3, all of them cubic [29]. The aging-in-air effects are usually less intense. However, the CO_2 and H_2O uptakes normally exceed the monolayer, thus suggesting that even for the heaviest lanthanide sesquioxides aging phenomena cannot be considered as purely surface processes. The IR spectra, and the absence of XRD diffraction lines other than those due to the starting cubic oxides suggest that the aged phases probably consist of a few layers thick amorphous hydrated carbonate coexisting with an oxide nucleus [29].

As revealed by the TG and TPD-MS diagrams reported in [29], the thermal stability of the aged phases also shows significant differences. It generally decreases throughout the lanthanide series. As a rough indication, heating, in a flow of inert gas, at temperatures as high as 973–1073 K would be recommended for cleaning the light aged-in-air oxides, like lanthana or neodymia, whereas 873 K would be high enough for the heaviest ones [15]. In the case of non-reducible light rare earth oxides, like lanthana, heating in a flow of H_2 may allow the elimination of the carbonate-containing phase at significantly lower temperatures. Carbonate species become fully reduced at about 873 K, CO and CH_4 being the major gaseous reduction products [33].

To summarize, the experimental studies commented on above show that aging-in-air is very relevant in the chemistry of the lanthanide sesquioxides. Both, the intensity of the process and the actual nature of the aged phases are kinetically controlled. Consequently, the rare earth oxides exhibit a rich variety of behaviors, far more complex than presumed on the basis of purely thermodynamic considerations. In this respect, it is worth recalling that, after [12], for processes implying no change in the oxidation state of the lanthanoid elements, smooth variations of behavior throughout the series should be expected to occur. This does not seem to be the case for the aging-in-air processes. In fact, different samples of the same oxide may show markedly differences of behavior.

The structural nature of the oxides plays a key role in determining their aging mechanism. Hexagonal and monoclinic oxides would behave similarly, which might well be understood in terms of their structural analogy [35,36]. For the cubic oxides two distinct behaviors could be observed as a function of the position of the lanthanoid element in the series. Likewise, differences in the rate and intensity of aging may be noted as a function of the preparation procedure and/or pre-treatments applied to the cubic oxides [37].

3. Redox behavior of the higher rare earth oxides

Upon reviewing the investigations carried out on the redox behavior of the so-called higher rare earth oxides, two major research lines may be distinguished. The first one has been focused on very fundamental aspects of this behavior: elucidation of the structural constitution of the different members of the homologous series of oxygen-deficient, fluorite-related phases, with generic formula Ln_nO_{2n-2m} [7,38,39], clarification of the complex phase diagram shown by these oxides [7,11,40], and characterization of the thermodynamic [11,41] and kinetic [42,43] aspects of the redox processes involving the different terms of the homologous series. These studies have recently been reviewed in refs. [1,44].

The second research direction has been mainly driven by one of the most successful industrial applications of ceria and ceria-based mixed oxides: their use as oxygen-storage materials in the three-way catalysis (TWC), the in-use technology for the abatement of exhaust emissions from gasoline-fuelled automobiles [45]. At present, TWC sales represent the 25% of the global catalyst market [46], thus explaining the spectacular increase of the research activities on ceria-based materials occurred in the last 20 years [47].

3.1. Redox behavior of the higher binary rare earth oxides

In accordance with the thermodynamic data reported in [11], ceria is by far the less reducible of the binary rare

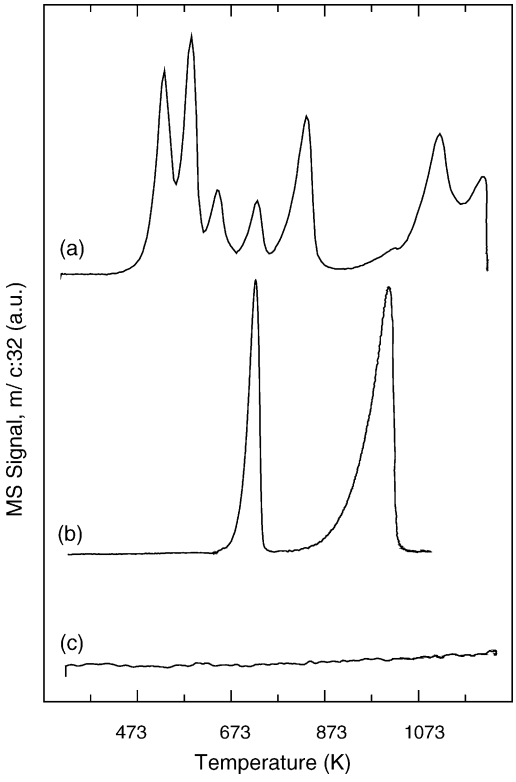

Fig. 3. TPD-MS traces for the oxygen ($m/e = 32$) evolved from praseodymia (a), terbia (b) and ceria (c), pre-treated as follows: heating under flowing 5% O_2/He at 973 K (1 h), cooling to 373 K under the same atmosphere, and further to 298 K in a flow of He. Experimental conditions for the TPD-MS run. Sample weight: 100 mg, flow of He: 60 $cm^3\ s^{-1}$, and heating rate: 10 K min^{-1}.

earth dioxides. In fact, CeO_2 may easily be prepared by calcination of a variety of precursor salts, whereas oxygen deficient praseodymia and terbia are always obtained by this procedure. Consequently, the actual stoichiometry of the latter oxide phases may significantly vary as a function of the specific preparation conditions: temperature and time of treatment, oxygen partial pressure and cooling conditions. Likewise, the specific pre-treatment conditions applied to praseodymia [48] and terbia [49] samples in order to clean them prior to any further experiment may significantly modify their actual redox state.

The different reducibility of the three binary oxides above is clearly shown in Fig. 3, where TPD-MS diagrams recorded for the oxidized forms of them are reported.

As deduced from Fig. 3, heating in a flow of inert gas induces a slight reduction of ceria, whereas praseodymia and terbia become fully reduced to sesquioxides. In the case of terbia, full reduction to Tb_2O_3 occurs below 1223 K, even under flowing 5% O_2/He [50]. The first oxygen peak in TPD-MS diagram for terbia (Fig. 3b) may be interpreted as due to the reduction of the δ phase ($TbO_{1.818}$) to the ι phase ($TbO_{1.714}$), the second one being assigned to the decomposition of $TbO_{1.714}$ to sesquioxide $TbO_{1.500}$ [49]. The intensity of first peak is sensitive to the pre-treatment conditions [49].

For praseodymia, the reduction in a flow of inert gas is far more complex implying several resolved steps, Fig. 3a. The first reduction peak, which may be interpreted as due to the decomposition of β to δ phase, is observed at 530 K; whereas the last one, that assigned to the decomposition of the ι phase (Pr_7O_{12}) to Pr_2O_3, takes place at approximately 1210 K, a temperature significantly higher than that observed on terbia for the same process. As in the case of terbia, the intensity of the low temperature peaks, and even the number of them, in the TPD trace for praseodymia may be strongly modified by the specific pre-treatment applied to the oxide sample [48].

In recent years, temperature programmed reduction is probably the most commonly used technique for routine redox characterization of these materials, particularly in the case of ceria and ceria-based mixed oxides. Hydrogen is by far the most usual reducing agent [51]. Mass spectrometry and thermal conductivity detectors (TCD) have been used as analytical devices [51]. TCD detectors may only account for hydrogen consumption, whereas MS may provide simultaneous information on the evolution of both hydrogen ($m/e = 2$) and water ($m/e = 18$). This is a relevant difference because H_2 and H_2O traces may not be identical, as implicitly is assumed in the usual interpretation of the TPR–TCD diagrams [51,52]. This is particularly true in TPR studies on NM/CeO_2 catalyst. Throughout a TPR experiment, two distinct, not necessarily coupled [52], processes may occur: hydrogen chemisorption on the oxide, which is strongly favored by the presence of highly dispersed noble metals (spillover), and creation of oxygen vacancies with inherent water evolution [51]. TPR–TCD devices do not discriminate between these two contributions to the total hydrogen consumption. Moreover, MS may also detect the formation of CH_4 or CO resulting from the reduction of carbonate species often trapped in the bulk of these oxides [53].

Compared to the TPD traces in Fig. 3, TPR-MS peaks are significantly shifted towards lower temperatures, the reduction to Ln_2O_3 of PrO_{2-x} and TbO_{2-x} samples being accomplished below 873 K [15]. Likewise, the different steps of terbia and praseodymia reduction become much poorly resolved [15].

The TPR traces for high surface area ceria samples typically show two major features peaking, under flowing 5% H_2/Ar, at approximately 650 and 1100 K [52]. These peaks are classically interpreted as due to a relatively fast surface process followed by a much slower diffusion of the oxygen vacancies into the bulk of the oxide [54]. This interpretation, however, has been recently revised [55]. According to [55], bulk reduction of ceria is not controlled by the diffusion step, differences in the thermodynamic properties of the ceria micro-crystals, as a function of their size and the oxide sintering occurring during the experiment, being the determining factors of the shape of the TPR diagram.

Full ceria reduction to Ce_2O_3 can hardly be achieved under the usual TPR conditions, prolonged (5 h) reduction treatments at 1223 K, in a flow of pure H_2, leading to 85% reduction to sesquioxide [15]. Under these strongly reducing

conditions, XRD studies have clearly shown the formation of the hexagonal phase, A-Ce_2O_3 [56].

Information about the re-oxidation behavior of the pre-reduced higher rare earth oxides is also available [11,50,56,57]. For ceria reduced at or below 773 K, re-oxidation occurs rapidly and to a large extent at room temperature. For higher reduction temperatures, full re-oxidation can only be accomplished upon heating the sample under oxygen [57]. The TPO study of heavily reduced ceria (T_{redn} = 1223 K) shows the occurrence of a change in the re-oxidation mechanism. This change has been interpreted as due to the formation of the hexagonal A-Ce_2O_3 [57]. The interpretation is consistent with the activation energy data reported for the re-oxidation of both hexagonal (210 kJ/mol) and cubic (105 kJ/mol) Pr_2O_3 [11]. For cubic Tb_2O_3, TPO data indicate that re-oxidation mainly occurs above room temperature [50], thus suggesting that re-oxidation is slower than on the fluorite-related oxygen-deficient ceria.

3.2. Modification of the redox behavior of the higher rare earth oxides

The redox properties of higher rare earth oxides may be significantly modified by a number of factors. Among them, the effect of noble metals (NM) highly dispersed on their surface, and the incorporation of aliocations into the oxide lattice, especially ceria, have been extensively investigated.

As revealed by the numerous TPR studies carried out on NM/CeO_2 samples, the presence of supported noble metals very much enhances the reducibility of the oxide [51]. This effect is acknowledged to be due to the low-temperature activation of hydrogen molecules on the surface of the metal crystallites, and the subsequent transfer of H atoms onto the oxide supports (spillover) [51]. As discussed in [51], however, the interpretation of TPR diagrams should be carefully analyzed in order to prevent a misleading interpretation of the hydrogen consumption peaks, which, as already noted in this work, not necessarily implies oxygen abstraction with inherent creation of oxygen vacancies.

The redox properties of the higher rare earth oxides may also be strongly modified by alio-cations forming mixed oxides with them. Considerable effort has been devoted to this family of fluorite-related oxides; most of this work being related to the development of new, more efficient, materials for applications as catalyst [45] or ionic conductors [58]. Though several other systems have been studied [15], ceria-zirconia is by far the most investigated one [2]. The incorporation of ceria-zirconia in TWC formulations has represented a major breakthrough in the development of this technology. Compared to bare ceria, CeO_2–ZrO_2 mixed oxides show better textural stability, enhanced redox activity, which has been interpreted as due to the higher oxygen mobility in the mixed oxide lattice [59]. They also show better resistance against redox deactivation induced by thermal aging [59]. In spite of these advantages, the redox response of ceria–zirconia may be reversibly modified by the thermo-chemical aging conditions [60,61]. Though a number of factors have been considered to play a role in determining this very peculiar effect [46,61–63], its precise origin is still unclear [64].

Acknowledgments

This work has been supported by the MCYT (Project MAT2002-02782), and the Junta de Andalucía (Groups FQM-110 and FQM-334).

References

[1] G. Adachi, N. Imanaka, Chem. Rev. 98 (1998) 1479–1514.
[2] A. Trovarelli (Ed.), Catalysis by Ceria and Related Materials, Imperial College Press, London, 2002.
[3] G. Adachi, N. Imanaka, Z. Kang (Eds.), Binary Rare Earth Oxides, Kluwer Academic Publishers, Amsterdam, 2004.
[4] T. Uda, K.T. Jacob, M. Hirasawa, Science 289 (2000) 2326–2329.
[5] D.J. Fray, Science 289 (2000) 2295–2296.
[6] J.E. Huheey, E.A. Keiter, R.L. Keiter, Inorganic Chemistry Principles of Structure and Reactivity, fourth ed., Harper Collins College Publishers, New York, 1993.
[7] Z.C. Kang, L. Eyring, Aust. J. Chem. 49 (1997) 981–996.
[8] L.R. Morss, J. Less Common Met. 93 (1983) 301–321.
[9] E.H.P. Cordfunke, R.J.M. Konings, Thermochim. Acta 375 (2001) 65–79.
[10] M.W. Shafer, J.B. Torrance, T. Penney, J. Phys. Chem. Solids 33 (1972) 2251.
[11] L. Eyring, in: K.A. Gschneider Jr., L. Eyring (Eds.), Handbook of the Physics and Chemistry of Rare Earths, North-Holland Publishing Company, 1979, pp. 337–399.
[12] D.A. Johnson, J. Chem. Educ. 57 (1980) 475–477.
[13] E. Antic-Fidancev, J. Holsa, M. Lastusaari, J. Alloys Compd. 341 (2002) 82–86.
[14] M.P. Rosynek, Catal. Rev. Sci. Eng. 16 (1977) 111–154.
[15] S. Bernal, G. Blanco, J.M. Gatica, J.A. Pérez Omil, J.M. Pintado, H. Vidal, in: G.A. Adachi, N. Imanaka, Z. Kang (Eds.), Binary Rare Earth Oxides, Kluwer/Academic/Plenum Press, 2004, chapter 2, p. 9–55.
[16] D.F. Mullica, W.O. Milligan, J. Inorg. Nucl. Chem. 42 (1980) 223–227.
[17] G.W. Beall, W.O. Milligan, H.A. Wolcott, J. Inorg. Nucl. Chem. 39 (1977) 65–70.
[18] J.A.K. Tareen, T.R.N. Kutty, Proc. Indian Acad. Sci. Chem. Sci. 89 (1980) 277–282.
[19] M.W. Shafer, R. Roy, J. Am. Ceram. Soc. 42 (1959) 563–570.
[20] R.P. Turcotte, J.O. Sawyer, L. Eyring, Inorg. Chem. 8 (1969) 238–246.
[21] H. Hinode, R. Sharma, L. Eyring, J. Solid State Chem. 84 (1990) 102–117.
[22] R.G. Charles, J. Inorg. Nucl. Chem. 27 (1965) 1489.
[23] J.A.K. Tareen, M.N. Viswanathiah, N. Krishnankutty, Rev. Chim. Min. 17 (1980) 50–57.
[24] G.W. Beall, W.O. Milligan, S. Mroczkowski, Acta Crystallogr. B 32 (1976) 3143–3144.
[25] J.M. Haschke, L. Eyring, Inorg. Chem. 10 (1971) 2267.
[26] A.N. Christensen, Acta Chem. Scand. 27 (1973) 2973–2982.
[27] A.N. Christensen, R.G. Hazell, Acta Chem. Scand. Ser. A-Phys. Inorg. Chem. 38A (1984) 157–161.
[28] T.R.N. Kutty, J.A.K. Tareen, I. Mohammed, J. Less Common Met. 105 (1985) 197–209.
[29] S. Bernal, F.J. Botana, R. García, J.M. Rodríguez-Izquierdo, React. Solids 4 (1987) 23–40.

[30] S. Bernal, F.J. Botana, R. García, J.M. Rodríguez-Izquierdo, J. Chem. Soc., Dalton Trans. (1988) 1765–1771.
[31] S. Bernal, F.J. Botana, R. García, J.M. Rodríguez-Izquierdo, Mater. Lett. 6 (1987) 71–74.
[32] S. Bernal, F.J. Botana, R. García, J.M. Rodríguez-Izquierdo, J. Mater. Sci. 23 (1988) 1474–1480.
[33] S. Bernal, F.J. Botana, R. García, F. Ramírez, J.M. Rodríguez-Izquierdo, J. Chem. Soc., Faraday Trans. I 83 (1987) 2279–2287.
[34] S. Bernal, F.J. Botana, R. García, J.M. Rodríguez-Izquierdo, Thermochim. Acta 66 (1983) 139–145.
[35] D.T. Cromer, J. Phys. Chem. 61 (1957) 753–755.
[36] H.L. Yakel, Acta Crystallogr. B 35 (1979) 564–569.
[37] R. Alvero, A. Bernal, I. Carrizosa, J.A. Odriozola, J.M. Trillo, J. Therm. Anal. 32 (1987) 637–643.
[38] R.L. Martin, J. Chem. Soc., Dalton Trans. (1974) 1335–1350.
[39] C. López-Cartes, J.A. Pérez-Omil, J.M. Pintado, J.J. Calvino, Z.C. Kang, L. Eyring, Ultramicroscopy 80 (1999) 19–39.
[40] Z.C. Kang, L. Eyring, J. Alloys Compd. 249 (1997) 206–212.
[41] L.R. Morss, in: K.A. Gschneidner, L. Eyring, G.R. Choppin, G.H. Lander (Eds.), Handbook on the Physics and Chemistry of Rare Earths, vol. 18, Elsevier Science, New York, 1994, pp. 239–291.
[42] A. Maren, S.H. Lin, R.H. Langley, L. Eyring, J. Solid State Chem. 53 (1984) 329–343.
[43] C. Boulesteix, L. Eyring, J. Solid State Chem. 71 (1987) 458–465.
[44] A. Trovarelli, in: A. Trovarelli (Ed.), Catalysis by Ceria and Related Materials, Imperial College Press, London, 2002, pp. 15–50.
[45] J. Kaspar, P. Fornasiero, N. Hickey, Catal. Today 77 (2003) 419–449.
[46] J. Kaspar, P. Fornasiero, J. Solid State Chem. 171 (2003) 19–29.
[47] A. Trovarelli, C. Leitenburg, M. Boaro, G. Dolcetti, Catal. Today 50 (1999) 353–367.
[48] Y. Takasu, M. Matsui, H. Tamura, S. Kawamura, Y. Matsuda, I. Toyoshima, J. Catal. 69 (1981) 51–57.
[49] Y. Takasu, T. Yoko-o, M. Matsui, Y. Matsuda, I. Toyoshima, J. Catal. 77 (1982) 485–490.
[50] S. Bernal, G. Blanco, F.J. Botana, J.M. Gatica, J.A. Pérez Omil, J.M. Pintado, J.M. Rodríguez-Izquierdo, J. Alloys Compd. 207/208 (1994) 196–200.
[51] S. Bernal, J.J. Calvino, J.M. Gatica, C. López-Cartes, J.M. Pintado, in: A. Trovarelli (Ed.), Catalysis by Ceria and Related Materials, Imperial College Press, London, 2002, pp. 85–168.
[52] M. Boaro, M. Vicario, C. de Leitenburg, G. Dolcetti, A. Trovarelli, Catal. Today 77 (2003) 407.
[53] F.M.Z. Zotin, L. Tournayan, J. Varloud, V. Perrichon, R. Frety, Appl. Catal. 98 (1993) 99.
[54] J. El Fallah, S. Boujana, H. Dexpert, A. Kiennemann, J. Majerus, O. Touret, F. Villain, F. Le Normand, J. Phys. Chem. 98 (1994) 5522.
[55] F. Giordano, A. Trovarelli, C. de Leitenburg, M. Giona, J. Catal. 193 (2000) 273.
[56] V. Perrichon, A. Laachir, G. Bergeret, R. Frety, L. Tournayan, O. Touret, J. Chem. Soc., Faraday Trans. 90 (1994) 773–781.
[57] S. Bernal, G. Blanco, M.A. Cauqui, G.A. Cifredo, J.M. Pintado, J.M. Rodríguez-Izquierdo, Catal. Lett. 53 (1998) 51–57.
[58] G. Adachi, N. Imanaka, S. Tamura, Chem. Rev. 102 (2002) 2405–2429.
[59] J. Kaspar, P. Fornasiero, M. Graziani, Catal. Today 50 (1999) 285–298.
[60] R.T. Baker, S. Bernal, G. Blanco, A.M. Cordon, J.M. Pintado, J.M. Rodriguez-Izquierdo, F. Fally, V. Perrichon, Chem. Commun. (1999) 149–150.
[61] S. Otsuka-Yao-Matsuo, T. Omata, N. Izu, H. Kishimoto, J. Solid State Chem. 138 (1998) 47–54.
[62] P. Fornasiero, T. Montini, M. Graziani, J. Kaspar, A.B. Hungría, A. Martínez-Arias, J.C. Conesa, Phys. Chem. Chem. Phys. 4 (2002) 149–159.
[63] T. Montini, M.A. Bañares, N. Hickey, R. Di Monte, P. Fornasiero, J. Kaspar, M. Graziani, Phys. Chem. Chem. Phys. 6 (2004) 1–3.
[64] S. Bernal, G. Blanco, J.J. Calvino, J.M. Gatica, J.A. Pérez-Omil, J.M. Pintado, Top. Catal. 28 (2004) 31–43.